ENGINEERING JOURNAL

Article

Diagnosis through Series Connected Photovoltaic Panels by Pulse Power Line Communication Technique

Pairote Sirinamaratana[a,*] **and Ekachai Leelarasmee**[b]

Department of Electrical Engineering, Faculty of Engineering, Chulalongkorn University, Bangkok 10330, Thailand
E-mail: [a]poppairote1@yahoo.com (Corresponding author), [b]ekachai.l@chula.ac.th

Abstract. Automatic diagnosis through individual photovoltaic panel (PV) is especially required for hard to reach locations such as solar rooftop or exterior building. Therefore, a novel solution for diagnosing PV panels through their PV string is proposed. Our solution not only measures IV curve of PV panels, but it can also determine disconnected or loose location of power cable. Large pulse communication technique is used to implement this solution to achieve low cost and zero power shut down. Comparison with other existing solutions is also discussed. The proposed technique is implemented on a five-panel PV string. Its satisfactorily testing results are presented under strong and weak sunlight conditions. For further understanding in PV panel, an amorphous silicon PV panel is characterized and also modeled to be a simple equivalent circuit.

Keywords: Photovoltaic panel, diagnosis, pulse, power line communication, modelling.

1. Introduction

Over the last decade, photovoltaic (PV) farms have tremendously increased worldwide [1] because of advances in its technology and incentive policies for renewable energy systems. Most of PV systems are connected to national AC power grid. Among many PV power plant topologies, the most widely used architectures are shown in Fig. 1. Note that a series connection of many PV panels is called as a "PV string". Centralized architecture [2] in Fig. 1(a) is cost effective topology. Multiple of PV strings are connected in parallel on high voltage DC bus to supply a DC/AC converter. In practical, if IV curve of a PV string in the centralized architecture is mismatch with other PV strings, it will effect on power generation. Therefore, the architecture is modified to be multi-string architecture [3] in Fig. 1(b). Each DC/DC converter, which has maximum power point tracking (MPPT) ability, is inserted between a PV string and HV DC bus to solve the PV string mismatch problem. Moreover, if some PV panels are damaged in the future and the used PV panel is obsolete, we can change some PV string to other available PV panels. However, the additional DC/DC converter also increases investment cost, which needs optimization over many trade-offs for economical design [3] such as power conversion efficiency, maintenance cost, upgradeability … etc.
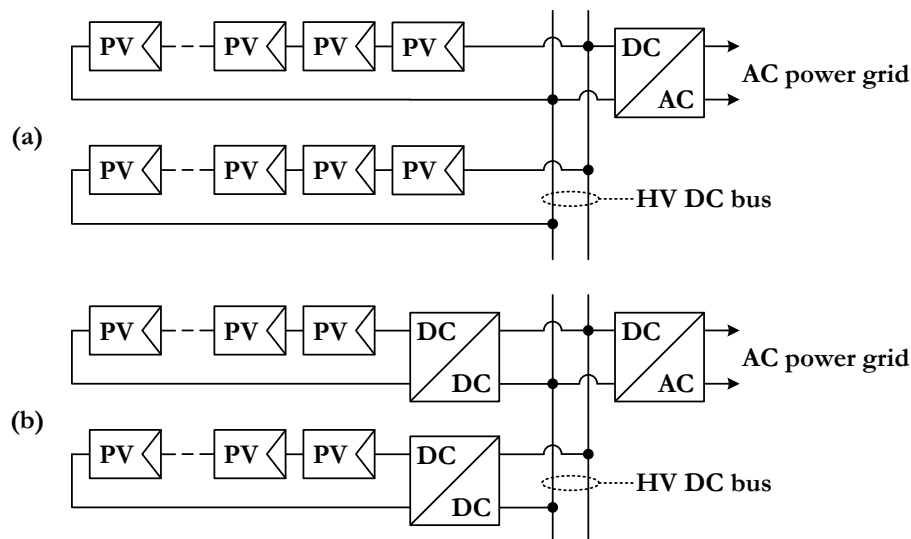

Fig. 1.   Traditional grid-connected PV systems (a) Centralized (b) Multi-string architectures.

PV   = PhotoVoltaic panel
DCU = Data Collector Unit
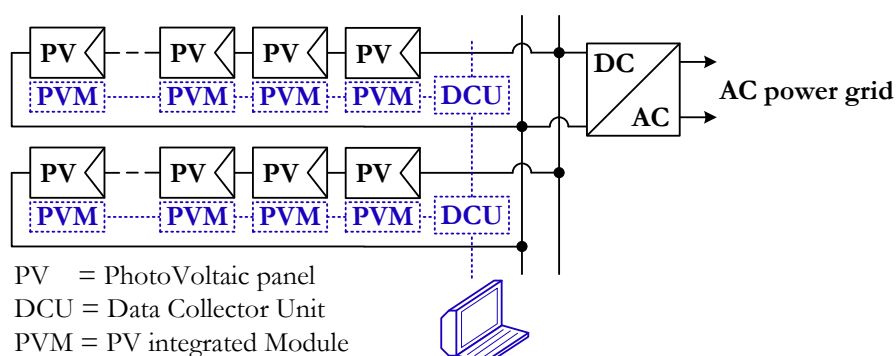PVM = PV integrated Module

Fig. 2.   An example of photovoltaic diagnostic system.

Generally, each power converter in solar farm can report its power in/out to a central computer. So, if there is a fault in a large solar farm, it can narrow down the fault location to within a converter. Then, an operator will manually search [4] for the faulty panel by using volt-meter, infrared camera and IV curve analyzer. This procedure is tedious and time consuming, especially for hard to reach locations such as solar rooftop or exterior building. So, automatic diagnosis is required. To implement this, a PV integrated module (PVM) is attached in each PV panel as shown in Fig. 2. Each PVM has its own unique ID (UID) for

identification. It measures and sends its PV panel's parameters to a data collector unit (DCU); and then to a central computer.

This paper proposes a new form of diagnosis solution through a PV string by using large pulse communication. Not only diagnosis, our proposed technique is also low cost and achieves zero power shut down. Content of this paper is organized as follows. In section 2, we will survey through existing solutions. Our technique, including with its implementation circuit, is proposed in section 3 and 4. Comparison with existing solutions will be discussed in section 5.Follow by experimental results and conclusion in section 6 and 7 respectively.

2. Survey of Existing Solutions

PV integrated modules (PVM) in Fig. 2 can communicate with DCU by using various methods such as additional wires [5], wireless communication network [6-9] and power line communication (PLC). Conventional PLC, which modulates carrier frequency into DC power line, is implemented for PV monitoring [10-12]. This technique is still costly since it requires a special purpose PLC IC and a switching regulator to convert 40V-90V of PV panel to supply the PLC IC at 3V-5V. Therefore, a small pulse PLC transmitter [13] is proposed to achieve low cost; however, its PLC receiver is still high cost to overcome switching noise on power line. Although these solutions [5-13] propose ways to check PV panel performance, there are some solutions [14, 15] that can do more. They can also determine sequence of PVM's UID in PV string automatically as well as locating disconnected or loose connection of power cable. These solutions are further described in details as follows.

A patented diagnostic solution [14] is shown in Fig. 3 where a data collector unit (DCU) is attached at a power converter and a PVM is attached on every PV panel in a PV string. It has 5 input/output wires for 5V supply bus, control (Ctrl) bus, Vref, data IN/ OUT and ground (GND). The 5V supply bus is sourced from DCU. Each PVM has a voltage to frequency (V2F) module to convert panel voltage to pulse frequency that goes through an optical coupler to a multiplexer (MUX). The MUX is controlled by a microcontroller (μC) to select data from V2F, μC or IN which receives OUT data from the next PVM. Hence V2F's frequency from all PVMs will reach DCU by controlling the MUX's appropriately.
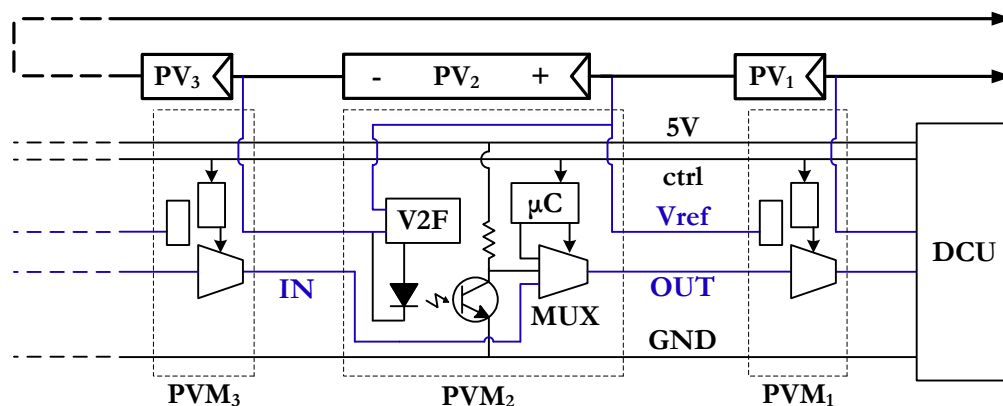

Fig. 3. Photovoltaic diagnostic solution of ref. [14].

Each PVM has its own unique ID (UID) for identification. DCU can determine PVM's UID sequentially by sending an UID request command through the Ctrl line. Each PVM in PV string will get the command simultaneously; then send its UID via its MUX. Therefore, DCU will get PVM_1's UID as the first ID because OUT port of PVM_1 is connected to DCU. Then, DCU asks PVM_1 to bypass IN to OUT in order to get UID of PVM_2. This procedure is repeated until the DCU get all PVM's UID.

Another feature of this system is its capability to detect loose or disconnected power cable. Notice that V2F of PVM_2 in Fig. 3 probes voltage between PV_2+ and PV_3+ (not PV_2-). If this voltage drops significantly from its normal value while PV string is sourcing current, it implies that PV_2 may have a problem or power cable connector between PV_2 and PV_3 has high resistance or is loose.

A major drawback of this technique is that its communication wire is connected in serial. Any cut on the wire will disrupt data communication. So, this system is not suitable for hard to reach locations such as

solar rooftop or exterior building since cable repair is difficult. Moreover, the V2F consumes power all day because there is no provision for shut down mode.
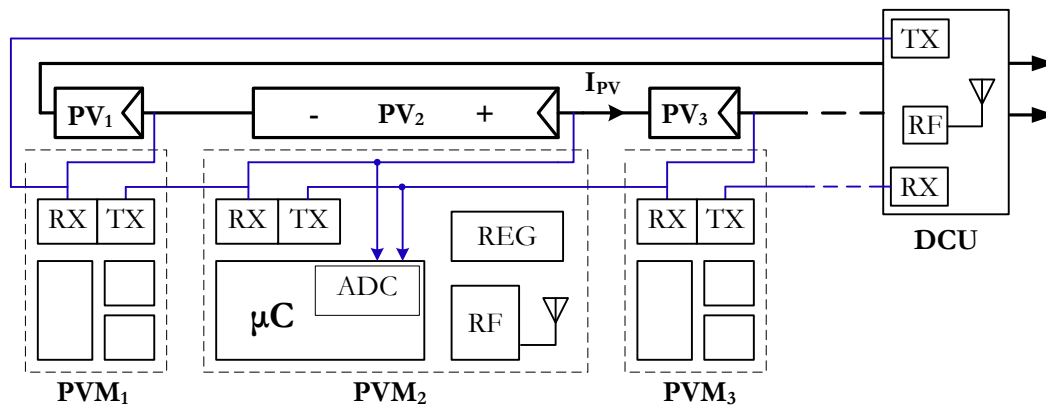

Fig. 4.   Photovoltaic diagnostic solution of ref. [15].

Another patented solution [15] is shown in Fig. 4. Here the PVM is powered by PV panel via its regulator (REG). Built-in analog to digital converter (ADC) inside μC measures PV panel's voltage, temperature and transmits these data via wireless communication network (RF). This solution adds one wire connecting TX block of a PVM to RX block of the next PVM to perform serial loop communication from DCU to PVM_1, PVM_1 to PVM_2 ... until last PVM back to DCU. Therefore, it can determine sequence of PVM's UID in PV string automatically.

Moreover, each PVM not only measures voltage of its PV panel, but also measure voltage of the next PV panel via the additional wire, such as PVM_2 can measure both V_{PV2} and V_{PV3}. This redundant V_{PV} measurement can be used to detect power cable disconnection or looseness which will be explained later in section 4.4.

A drawback of this solution is that its wireless communication network transceiver (RF) and switching regulator (REG) [6] add up the cost significantly, and no provision for shut down mode.

3.   The Proposed Solution

In PV power plant, measuring of individual PV panel is not required frequently. Measuring only a few times per day are enough to check the panel's degradation, dirt or loose connection. Diagnosis through PV string may only be required when a power converter reports its output power drop. So, PVM on each PV panel should be able to go to shut down mode. Hence, our goal is to design a new PVM which has zero power shut down and also low cost.
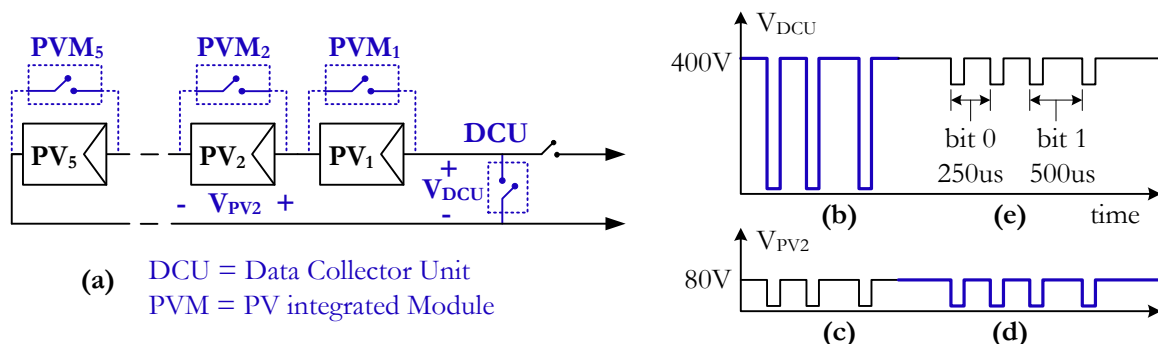

Fig. 5.   (a) Concept of the proposed Pulse Power Line Communication (P-PLC); pulses (b) generated by toggling the DCU's switch 3 times give rise to pulses (c) at PV_2; and pulses (d) generated by toggling PV_2's switch 4 times give rise to pulses (e) at DCU.

3.1. Pulse Power Line Communication (P-PLC)

Figure 5 shows the basic concept of our proposed solution [16] using a five-panel PV string as an example. Here a switch is placed across each PV panel and DCU. If PV panel's voltage (V_{PV}) is 80V, voltage across the DCU (V_{DCU}) will be 400V. By closing the switch at DCU for 10 µs and opening, a 400V negative pulse is created at the DCU as shown in Fig. 5(b). This pulse will propagate through the power line and appear equally across all PV panels as a negative 80V pulse as shown in Fig. 5 (c). Hence DCU can toggle its switch to transmit data to all PVs. Alternatively, a 10 µs closing switch across a PV panel will generate a negative 80V pulse at its own terminals and the DCU as shown in Fig. 5 (d) and (e), but not at any other PV panel. Therefore, there is no direct communication between PVMs. DCU must act as a master unit to control data flow. We call this type of communication as pulse power line communication or P-PLC. By the way, data coding is easily defined by duration between consecutive pulses as shown in Fig. 5(e), i.e. 250µs for bit '0' and 500µs for bit '1'.
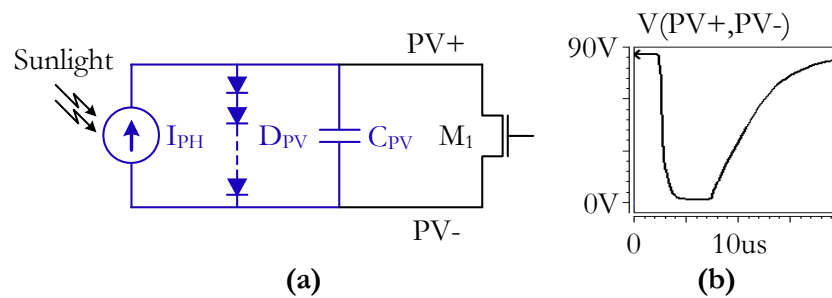

Fig. 6.   (a) Simplified PV panel model; (b) its pulse generated by switch M_1.

To understand the pulse generation, equivalent circuit of a PV panel [17, 18] is shown in Fig. 6(a) where I_{PH} is photo generated current, D_{PV} represents the PN junction of solar cell, C_{PV} represents depletion and diffusion capacitance of the PN junction. Maximum I_{PH} is 1A - 5A depending on PV panel size. When the switch M_1 is turned on, C_{PV} is discharged, I_{PH} will flow through M_1 and the panel voltage drops to zero quickly as shown in Fig. 6(b). Then, after the switch opens C_{PV} is charged by I_{PH} causing its panel voltage to ramp up with a slope of I_{PH}/C_{PV}. Hence, the ramp up time depends on I_{PH} or light intensity, which will be shown later in experimental results section.

3.2. The Pulse Power Line Communication (P-PLC) with Additional Wire
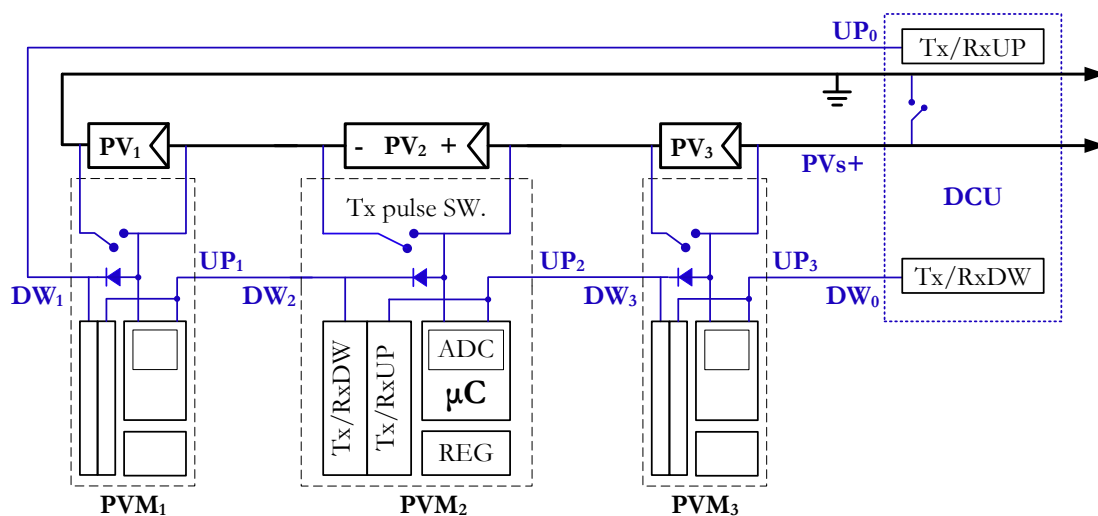

Fig. 7.   Block diagram of the proposed PV integrated module (PVM).

Although the P-PLC does not require extra wiring for data communication, it cannot locate DC power cable disconnection or determine sequence of PVM's UID in PV string automatically. Using an approach similar to [15] in Fig. 4, these features can be implemented by adding one in/out wire named UP and DW

as shown in Fig. 7 where the PVM structure is proposed. This wire together with the Tx/RxUP and Tx/RxDW modules forms a bidirectional serial communication between adjacent PVMs as a 2nd communication channel. The PVM is powered by PV panel via its regulator (REG). Built-in analogue to digital converter (ADC) inside microcontroller (µC)is used to measure PV panel's voltage. Moreover, each PVM not only measures voltage of its PV panel, but also measure voltage of the next PV panel via the additional wire, such as PVM_2 can measure both V_{PV2} and V_{PV3}. This redundant V_{PV} measurement can be used to detect power cable disconnection or looseness, or reduce failure possibility of V_{PV} measurement which will be explained later in section 4.4.
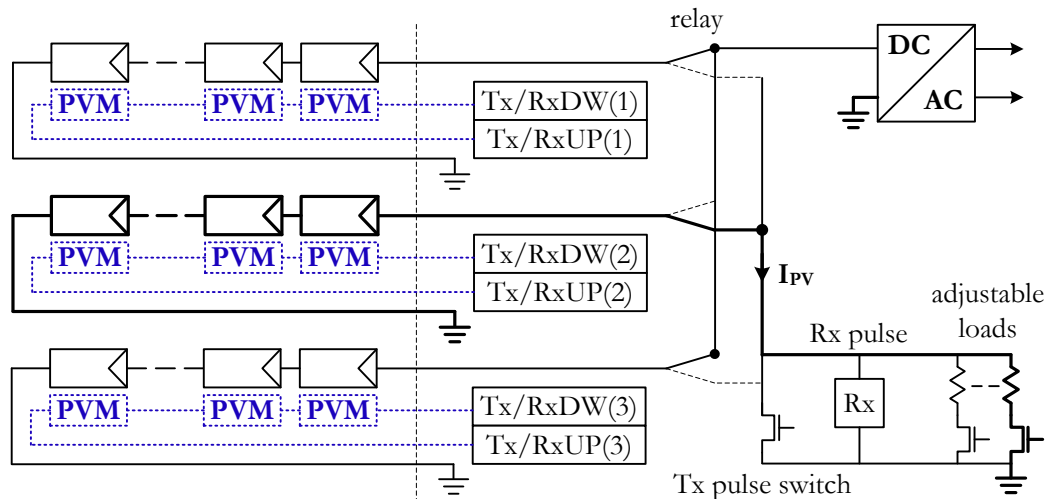

Fig. 8.   Block diagram of the proposed Data Collector Unit (DCU), attached at a power converter.

An example of DCU at a power converter is shown in Fig. 8. DCU can select a PV string by power relays (FTR-J2). Tx pulse switch and Rx pulse circuit are used to implement the P-PLC. The selected PV string will be loaded by adjustable loads [19, 20] to measure PV panels' IV curve. V_{PV} is measured on each PVM, whereas I_{PV} is measured on the DCU. Similar to the PVM, Tx/RxUP and Tx/RxDW blocks are also added in DCU for serial communication through each PV string.

4. Circuit Implementation

4.1.   Start Up and Shut Down Mechanism of the PVM

The circuit inside our proposed PVM is shown partially in Fig. 9. If there is no pulse communication for a long time such as more than 3ms, transistor Q_1 and Q_{L1} are opened and there is no DC path from node PV+ to node PV-. Hence the circuit that enters a shutdown mode will consume zero power. The pulse receiver in Fig. 9(a) performs two functions, to detect pulses from the DCU and to wake up the PVM from its shut mode. Its operation is as follows. D_1, C_1 and resistors at node 'A' form a pulse detector that turns on Q_1 at V_{PV} rising edge as depicted in Fig. 10. During this pulse, Q_1 is turned on allowing C_{HV} to be charged by PV+ through Q_{REG} and D_2. The voltage rises in C_{HV} depends on the pulse width generated by C_1 but will accumulate over consecutive pulses. Whereas +15V supply across C_{HV} is rising, the 5V regulator (5V Reg) is turned on and +5V supply is also rising too. Whenever the +5V supply reaches a threshold level of 3V at which Q_{L1} is turned on and latched (to be described later). As a result, GND and PV- are continuously connected together causing the 15V regulator to conduct and wake up the whole circuit. The GND and PV- connection or waking up of the latched switch $Q_{L1}$is shown in Fig. 11 between time 0 and 1ms where V(GND, PV-) goes down from V(PV+, PV-) to 0V. From now on, the 'Rx' output of the Pulse Rx circuit will be used by µC to decode DCU's pulses.
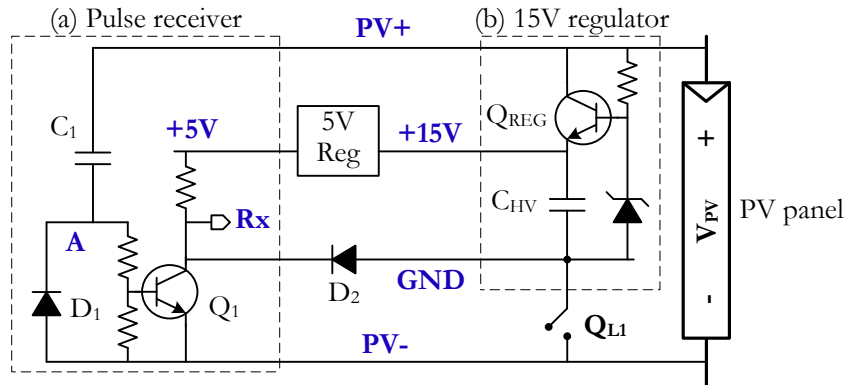
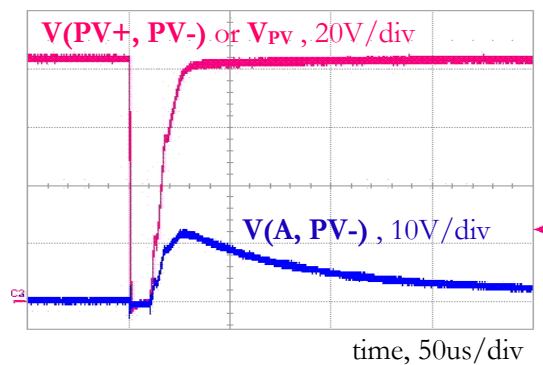Fig. 9.   (a) Pulse receiver and (b) 15V regulator circuits inside a PV integrated module (PVM).

Fig. 10. Input pulse V_{PV} or $V(V_{PV+}, V_{PV-})$ and the resulting positive edge detected waveform across $V(A, PV-)$.
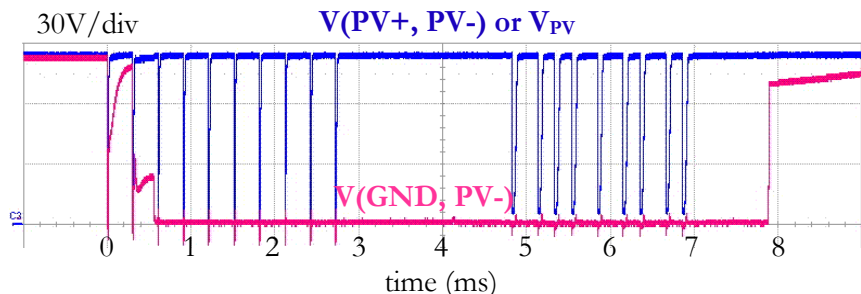

Fig. 11. GND and PV- are short together after 2 V_{PV} pulses and disconnected at 8ms by µC inside PVM.

The switch Q_{L1} belongs to the latch circuit as shown in Fig. 12(a). Node 'OFF' from a µC's port is an input, which is high impedance. Turn-on level of Q_{L1} is set to 3V (between +5V supply and GND) by Q_{L2} and the stacked diodes. Once being triggered on, Q_{L1} remains on until µC changes port direction from input to output, and forces node 'OFF' high (forces to +5V) to turn Q_{L1} off; putting the whole circuit back to shut down mode at 8ms in Fig. 11. Then,+5V supply (vs. GND) will go down until 1.8V, the µC will reset itself and µC port will change back to input port or high impedance again.

In conclusion, this proposed start up and shut down mechanism makes our PVM achieve zero power consumption in shut down mode without using expensive special-propose regulator IC.

4.2.   The 15V Regulator and Tx Pulse Switch

The 15V regulator in Fig. 9(b) regulates 40V - 90V of PV panel down to +15V supply and also +5V supply needed by microcontroller and the rest circuits. We use a simple linear regulator to achieve low cost. Its energy efficiency is irrelevant since the PVM seldom operates. The concern is power dissipation on Q_{REG} to become overheated. From data sheet, microcontroller (µC, ATmega 8) consumes 3 mA when operating at 5V and 1.8432 MHz clock. If a 90V PV panel is used, the regulator must dissipate 3mA×75V

= 225mW. Therefore, TO-220 transistor package is chosen for Q_{REG} (BUL128 or ST13005) because it has low thermal resistance 62.5C/W (junction to ambient). By simple estimation, temperature will increase 62.5C/W×225mW = 14C. If ambient temperature on backside of PV panel is 75C, the worst case temperature at Q_{REG} is 75C+14C = 89C which is still far from its operating limit of 125C.
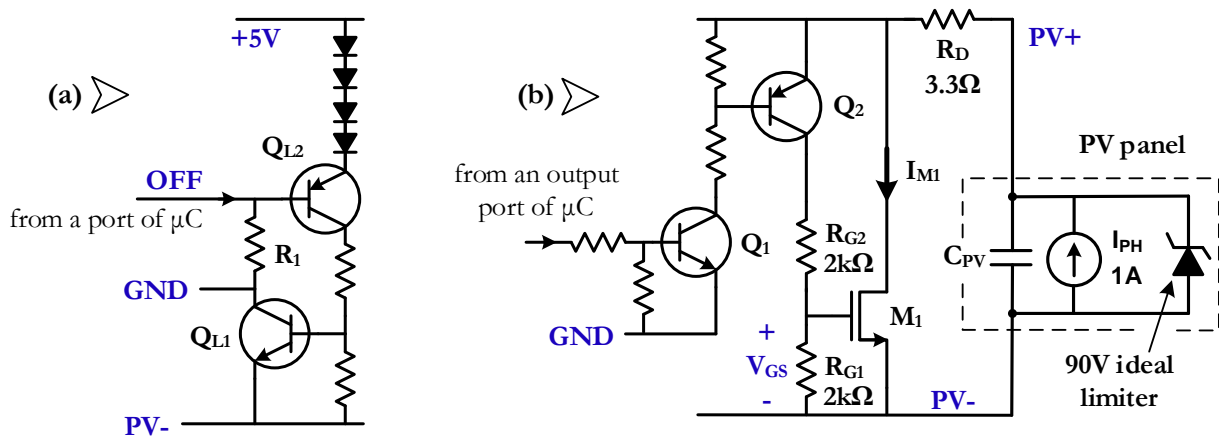

Fig. 12. (a) Circuit of the latched switch Q_{L1}; (b) Tx pulse switch circuit inside a PVM.

Figure 12(b) shows Tx pulse circuit where M_1 acts as a switch across the panel. It is controlled by 5V signal from μC. IRF630B, N-channel MOSFET (9A, V_{DS} 200V, V_{GS} ±30V) is chosen as M_1. It can endure inrush current up to 36A. While Q_1 and Q_2 turning off, R_{G1} pulls M_1 to turn off. Whenever Q_1 and Q_2 turned on, V_{GS} rising will be slow down by R_{G2} and M_1's C_{GS} delay, which prevents V_{GS} to not exceed ±30V. R_D is added to limit the inrush current from C_{PV} that will flow through M_1 after its sudden turning on. Finally, the Tx pulse circuit is simulated by spice simulator to ensure its operation as shown in Fig. 13.

The 50W PV panel in our test has capacitance at dark illumination or C_{J0}= 65nF. For simplicity and safety, higher values of linear C_{PV} (0.2uF and 1uF) are used in this simulation instead of real nonlinear C_{PV} which is further described in Appendix section. The simulation results indicate that 10us turning on time of the switch is enough to make a pulse, V_{GS}<10V, and inrush current (I_{M1}) < 20A.
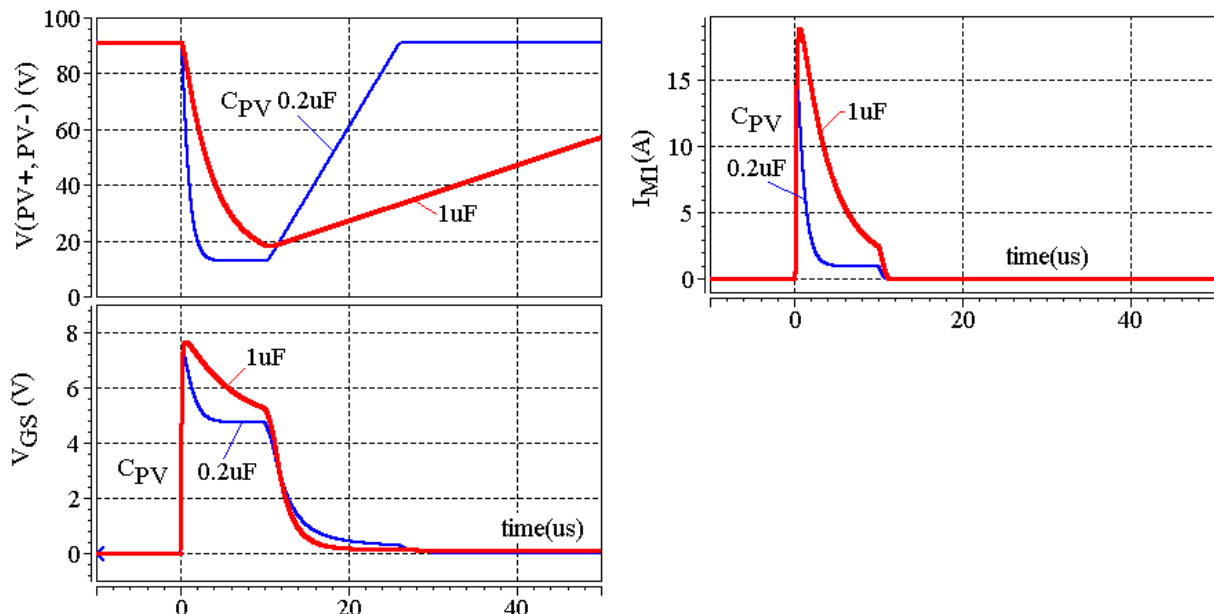

Fig. 13. Simulation results of the Tx pulse switch circuit.

4.3. Tx/RxUP and Tx/RxDW Circuits

The Tx/RxUP and Tx/RxDW blocks in Fig. 7 that implement the bidirectional serial communication between adjacent PVMs are now described. Figure 14(a) shows Tx/RxUP(1) circuit in PVM$_1$connecting

with Tx/RxDW(2) circuit in PVM$_2$. Both are augmented from the Pulse receiver circuit depicted in Fig. 9(a) by adding Q$_2$, D$_3$ and C$_2$. Denote that Q$_2$(1) is Q$_2$ in PVM$_1$. PVM$_1$ can send pulses to PVM$_2$ by turning on Q$_2$(1) that creates positive pulse on node A$_1$ in Tx/RxUP(1) as probed in Fig.14(b). The pulse will pass through C$_2$(1) and C$_2$(2) to make a positive pulse on node B$_2$ in Tx/RxDW(2) and turn on Q$_1$(2) switch for a short period of time. On the other hand, PVM$_2$ can also send pulses to PVM$_1$ by turning on Q$_2$(2). Therefore, it can do bidirectional serial communication. Notice that this communication channel does not create large pulse across PV panel as the P-PLC do. Therefore, it does not disturb power sourcing of PV panels.

Fig. 14.   (a) Tx/RxUP and Tx/RxDW circuits; (b) Probed voltages inside the circuits when Q$_2$(1) in PVM$_1$ generates a pulse.

4.4.   Redundant VPV Measurement

By built-in analog to digital converter (ADC) and 2.56V reference inside microcontroller (µC, ATmega 8), PVM$_1$ can measure V$_{PV1}$ across nodes PV$_1$+ and GND$_1$; and also V$_{PV1}$+V$_{PV2}$ across node UP$_1$ and GND$_1$ via the additional wire as shown in Fig. 14(a). It means that voltage of a PV panel can be redundantly measured by 2 PVMs.

The redundant measurement gives us 2 advantages. Firstly, we can detect power cable looseness from high resistance connector R$_{CONN}$ between PV$_1$ and PV$_2$. For example, if PV string's current or I$_{PV}$ = 0, the measured voltage of PV$_2$ by PVM$_1$ or V$_{PV2}$ by PVM$_1$= V$_{PV2}$ by PVM$_2$; and if I$_{PV}$> 0, voltage will drop across R$_{CONN}$, so V$_{PV2}$ by PVM$_1$< V$_{PV2}$ by PVM$_2$. This can imply that power connector between PV$_1$ and PV$_2$ has high resistance or loose. If power connector between PV$_1$ and PV$_2$ is disconnected, PVM$_1$ will measure V(UP$_1$, GND$_1$) = V$_{PV1}$, which differs from normal case that V(UP$_1$, GND$_1$) = V$_{PV1}$+V$_{PV2}$. Secondly, if failure possibility over 25 years of a PVM is 3%, the failure possibility of the redundant V$_{PV}$ measurement by 2 PVMs will greatly decrease to 3%✕3% = 0.09%.

5. Comparison with Existing Solutions

Table 1 shows capabilities of 5 existing solutions and our proposed solution. Solution [6] can measure open circuit voltage V_{OC} and short circuit current I_{SC} of a PV panel. It uses wireless network for communication. Solution [10] uses conventional PLC, modulating carrier frequencies into DC power line. Its PVM does not measure any PV panel parameter but can disconnect PV panel from its PV string and let string's current flow through a bypass diode. Current load varying and PV string's voltage measurement are taken by its master unit or DCU. Solution [13] implements a pulse PLC in which each PVM has only a low cost transmitter that periodically transmits data in form of small pulses. However, its DCU's pulse receiver is rather complicated and expensive since it has to overcome switching noise on power line. By the way, these above solutions do not have additional wire. So, they cannot determine sequence of PVM's UID in PV string automatically. They also cannot locate disconnected or loose connection of power cable, and don't have redundant mechanism to reduce failure possibility from out-of-order PVM. The patented solutions [14, 15] are already described in section 2.

Comparison to others, our proposed solution is low cost because it uses only simple circuits. It also has other salient properties such as line fault location, sequential PVM's UID, redundant V_{PV} measurement and most importantly zero power shut down mode.

Notice that solutions [13-15] continuously monitor operating PV panels, but our solution and [6, 10] will interrupt power generation of the selected PV string to allow measurement of many parameters such as open circuit voltage V_{OC}, short circuit current I_{SC} and IV curve of PV panels.

Table 1.   Capabilities of existing PV panel monitoring solutions and our proposed solution.

Capabilities	[6] RF	[10] PLC	[15] RF+wire	[13] pulse PLC	[14] wires	Proposed solution
Use additional wire	no	no	yes	no	yes	yes
Cost of PV integrated Module (PVM)	high from PLC IC or RF IC and switching regulator			low	lowest	low
Automatic PVM's UID ordering determination	no	no	yes	no	yes	yes
Can locate power cable loose or disconnection	no	no	yes	no	yes	yes
Redundant V_{PV} measurement	no	no	yes	no	no	yes
Shut down mode	no	no	no	no	no	yes
Power interruption while measuring	yes	yes	no	no	no	yes

6. Experimental Results

A string of 5 PV panels is set up to verify the concept of the proposed solution. Each panel is a 50W 63.5×124.5 cm² amorphous silicon PV panel (BS-50) as shown in Fig. 15. Tests are carried out at strong and weak sunlight at which the open circuit voltage V_{OC} and short circuit current I_{SC} are 86V, 735mA and 67V, 25mA respectively.

Fig. 15.   A five-panel PV string for our experiment.

Figure16 shows waveforms at data collector unit (DCU) when it switches for the first 3ms to wake up all PVMs; and response of a PVM starts sending pulses at 5ms. Although correctness of the operation is confirmed, the waveform at weak sunlight has a rise time of 200μs. Therefore, this slow rise time under the weak sunlight is set as our criteria for time interval between consecutive pulses as 250μs for bit '0' and 500μs for bit '1'; or data rate is at least 2k b/s.
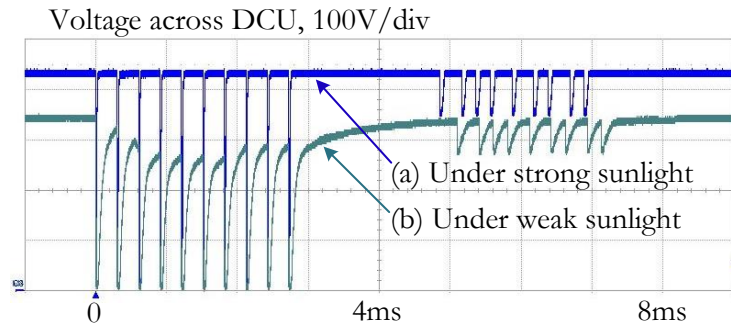

Fig. 16.   Pulses across data collector unit (DCU) under (a) strong sunlight and (b) weak sunlight.
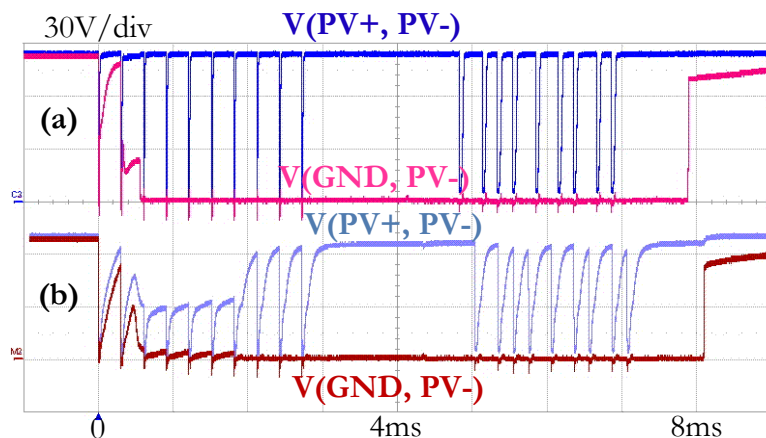
Fig. 17.   Waveforms across a PVM (a) under strong sunlight; (b) under weak sunlight.

Figure 17 shows waveforms at the responding PVM to illustrate how it is waken up before 3ms when GND is short to PV- or V(GND,PV-) = 0V under both (a) strong and (b) weak sunlight. Notice that V_{PV} under weak sunlight (b) drops at time between 0 – 2ms. This is due to the fact that some 25mA of I_{PH} inside the PV panel has to charge supply decoupling capacitor C_{HV} in PVM.

In order to measure IV curve of PV panel in a PV string. DCU will load a selected PV string by its adjustable current load [19, 20] as depicted in Fig. 8. An example of waveform at DCU, while measuring IV curve of PV panels in a PV string is probed as Fig. 18. It is divided into 4 steps.

(a) DCU sends a command to ask all PVMs in a selected PV string to measure V_{PV}.
(b) Then, DCU will increase its load in many steps. All PVMs in the string will synchronously measure V_{PV}.
(c) After the measurement finish, DCU will call a PVM to transmit its measured data to DCU.
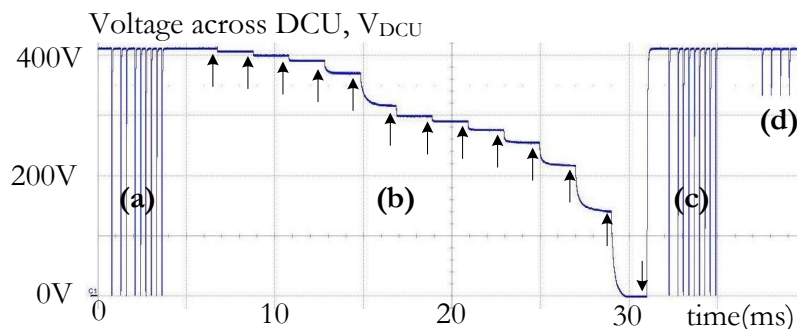(d) The called PVM sends its measured data to DCU.

Fig. 18. Probed voltages across DCU while measuring IV curve of PV panels in a PV string.

The measured IV curve of a PV panel is plotted in Fig. 19. Both curve (a) and (b) are tested under strong sunlight. Curve (a) is IV curve of a good PV panel, whereas curve (b) is IV curve of a partial shading PV panel.
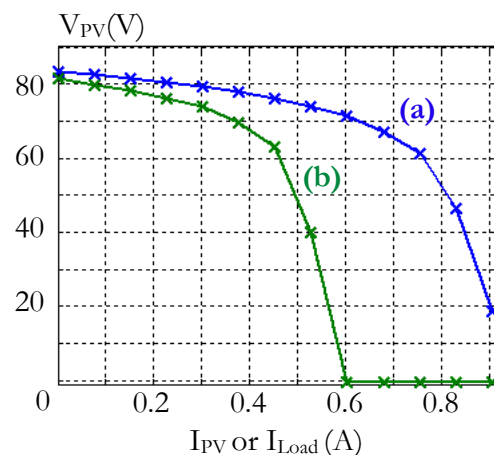

Fig. 19. Measured IV curves under strong sunlight from (a) a good PV panel (b) a partial shading PV panel.

7. Conclusions

This work presents a new solution to diagnose PV panels in a PV string. It introduces a new kind of communication called the pulse power line communication (P-PLC). Circuits of a PV integrated module (PVM) are designed to achieve low cost and zero power shut down. With one additional wire, our solution can detect fault location in the power cable and determine sequence of PVM's unique ID in PV string automatically. Under strong and weak sunlight, the experimental results show that data rate of P-PLC can be achieved at least 2k b/s.

Appendix—Photovoltaic panel characteristic and modeling

Although, this characterization bases on another 40W amorphous silicon PV panel (not the 50W amorphous silicon PV panel used in section 6), it could be enough to make understand PV panel behaviour.
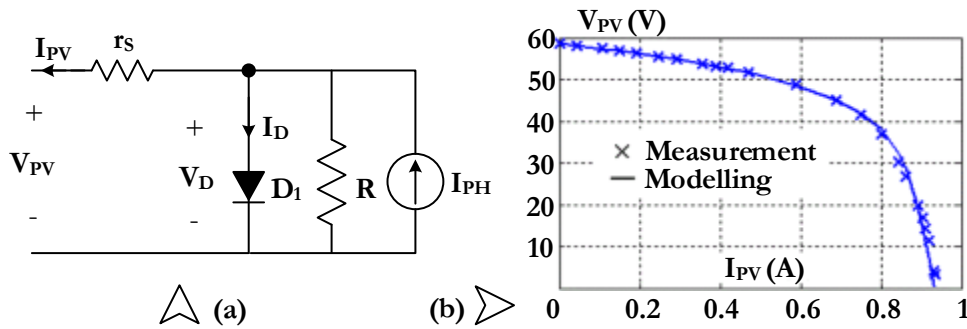
Fig. 20. (a) Equivalent circuit of PV panel [17, 18]; (b) IV curve of a 40W amorphous silicon PV panel.

Equivalent circuit of PV panel [17, 18] is shown in Fig. 20 (a). I_{PH} is photo generated current. D_{PV} represents the PN junction of solar cell. $C_{PV} = C_J + C_D$ where C_J is depletion capacitance and C_D is diffusion capacitance of the PN junction. By using level 1 diode model [21], D_{PV}, C_J and C_D can be expressed by equations as follow

$$I_D = I_0 \left(exp \left(\frac{V_D}{nV_T} \right) - 1 \right) \tag{1}$$

$$C_J = C_{J0} \left(1 + MJ \times \frac{V_D}{PB} \right) \tag{2}$$

$$C_D = TT \times \frac{\partial I_D}{\partial V_D} = TT \times \frac{I_D + I_0}{nV_T} \tag{3}$$

I_O is dark saturation current. n is diode quality factor. V_T is thermal voltage (0.0259 mV at 25C). MJ is area junction grading coefficient; its default value is 0.5. PB is area junction contact potential. TT is transit time. By using "lsqcurvefit" function in MATLAB, all DC parameters I_{PH}, I_0, n, R, r_S in the equivalent circuit in Fig. 20(a) and Eq. (1) are optimized to fit the measured IV data points in Fig. 20(b). The fitted curve is also plotted in Fig. 20(b), and the parameters are shown in Table 2.

Table 2. Calculated parameters in the circuit model of a 40W amorphous silicon PV panel.

I_{PH}	Photo current	0.94	A
I_0	Dark saturation current	170	μA
n	Diode quality factor	265	-
R	Parallel resistor	490	Ω
r_S	Series resistor	2.82	Ω
C_{J0}	Zero-bias junction capacitance, or capacitance at dark illumination	92.3	nF
TT	Transit time (τ_T)	7	us
PB	Junction contact potential	200	V

Capacitance of the PV panel is measured by test set up in Fig. 21(a). The PV panel (PV) is placed under a strong sunlight level. Vector network analyzer (VNA2180) is a tool to measure impedance of the PV panel. C_{BP}, a 5μF polypropylene capacitor, blocks DC voltage between the PV panel and the VNA. I_{PV} can be adjusted at V_G node of the constant current circuit. Heat sink of transistor M_2 must be dipped into water to sink power from the PV panel. Finally, a plot of measurement results between C_{PV} and V_{PV} is shown in Fig. 21(b). Frequency 50 kHz - 100 kHz is chosen to characterize C_{PV} because resistive part of PV panel's impedance will dominate its reactive part at frequency lower than 10 kHz. On the other hand, if we use frequency higher than 500 kHz, inductance from wiring inside the PV panel and our circuit connection will dominate C_{PV} value as shown in [11].
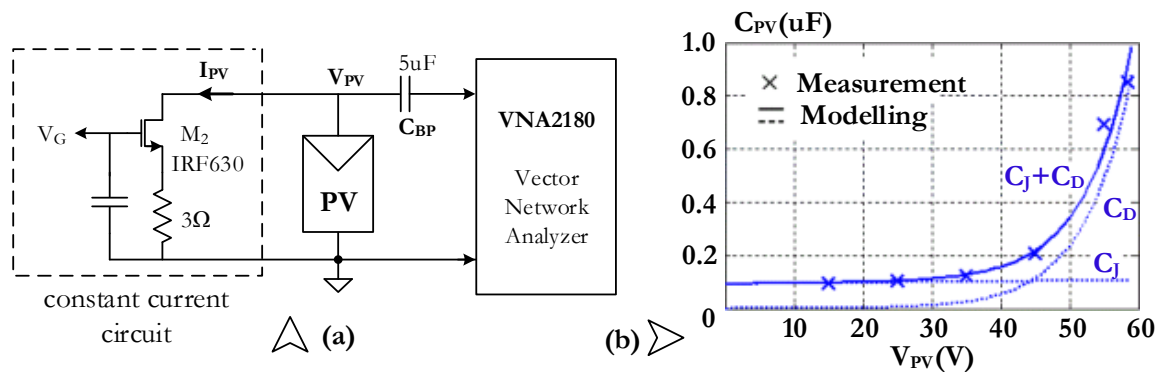
Fig. 21. (a) A test set up for IV curve and C_{PV} measurement; (b) Measurement results and modeling curve of C_{PV}.

From the measurement result which I_{PH} is constant, if we sink I_{PV} from the PV panel, V_{PV} and I_D will be decreased. I_D decreasing causes C_{PV} decreasing because C_D in Eq. (3) is proportional to I_D. By using "lsqcurvefit" function in MATLAB, CJ_0, TT and PB in Eq. (2) and (3) are optimized to fit the measured C_{PV} in Fig. 21(b). The fitted curve is also plotted in Fig. 21(b) and the parameters are shown in Table 2.

Acknowledgement

References

[1] P. Attaviriyanugap, "Status of renewable energy in Europe, U.S. and Japan and protection challenges in solar photovoltaic arrays," *Engineering Journal*, vol. 14, no. 3, pp. 57–70, Jul. 2010.

[2] Y. Zhao, J. F. dePalma, J. Mosesian, R. Lyons, and B. Lehman, "Line fault analysis and protection challenges in solar photovoltaic arrays," *IEEE Trans. on Industrial Electronics*, vol. 60, no. 9, pp. 3784–3795, Sep. 2013.

[3] Z. Moradi-Shahrbabak, A. Tabesh, and G. R. Yousefi, "Economical design of utility-scale photovoltaic power plants with optimum availability," *IEEE Trans. on Industrial Electronics*, vol. 61, no. 7, pp. 3399–3406, Jul. 2014.

[4] Z. Machacek, Z. Benda, and D. Busek, "Diagnostics of photovoltaic power plant operating," in *Proc. IETMediterranean conf. and Exhibition on Power Generation Transmission Distribution and Energy Conversion*, Agia Napa, Nov. 2010, pp. 1–4.

[5] J. D. Bennett and B. E. Garlick, "Solar panel monitoring system," US patent, US 2010/0043780 A1, Feb. 2010.

[6] P. Guerriero, V. d'Alessandro, L. Petrazzuoli, G. Vallone, and S. Daliento, "Effective real-time performance monitoring and diagnostics of individual panels in PV plants," in *Proc. Clean Electrical Power conf.*, Alghero, Jun. 2013, pp. 14–19.

[7] M. Gargiulo, P. Guerriero, S. Daliento, A. Irace, V. d'Alessandro, M. Crisci, A. Smarrelli, and M. Smarrelli, "A novel wireless self-powered microcontroller-based monitoring circuit for photovoltaic panels in grid-connected systems," in *Proc. IEEE Int. Symposium on Power Electronics Electrical Drives Automation and Motion (SPEEDAM)*, Jun. 2010, pp. 164–168.

[8] E. A. Kawam and E. A. Kawam, "Photo-voltaic solar array health monitor," US patent, US 2008/0306700 A1, Dec 2008.

[9] S. Kumar, P. M. Patel, and D. K.Bhana, "Smart device for enabling real-time monitoring, measuring, managing, and reporting of energy by solar panels and method therefore," US patent, US2010/0241375 A1, Sept. 2010.

[10] P. Jonke, C. Eder, J. Stockl, and M. Schwark, "Development of a module integrated photovoltaic monitoring system," in *Proc. IEEE Industrial Electronics Society conf. (IECON)*, Nov. 2013, pp. 8080–8084.

[11] P. Sirinamaratana, E. Leelarasmee, and W. Pora, "A series DC power line communication and its application to monitoring photo-voltaic strings," *Journal of Circuits Systems and Computers*, vol. 22, no. 9, Nov. 2013.

[12] E. Roman, R. Alonso, P. Ibanez, D. Goitia, and S. Elorduizapatarietxe, "Intelligent PV module for grid-connected PV systems," *IEEE Trans. on Industrial Electronics*, vol. 53, no. 4, pp. 1066–1073, 2006.

[13] H. Nosato, Y. Kasai, E. Takahashi, and M. Murakawa, "A very low-cost low-frequency PLC system based on DS-CDMA for DC power lines," in *Proc. IEEE International Symposium on Power Line Communications and its Applications*, Beijing, Mar. 2012, pp. 398–403.

[14] G. D. Hasenfus, "Smart sensors for solar panels," U.S. patent, US 2009/0140719 A1, Jun. 2009.

[15] G. E. Presher Jr and C. J. Warren, "System and method for monitoring photovoltaic power generation systems," US patent, US 2006/0162772 A1, Jul. 2006.

[16] P. Sirinamaratana and E. Leelarasmee, "Circuits for data communication through DC power line in solar farm," in *Proc. IEEE Electron Devices and Solid-State Circuits Conf*, Hong Kong, Jun. 2013, pp. 1–2.

[17] N. D. Benavides and P. L.Chapman, "Modeling the effect of voltage ripple on the power output of photovoltaic modules," *IEEE Trans. on Industrial Electronics*, vol. 55, no. 7, pp. 2638–2643, Jul. 2008.

[18] S. B. Adejuyigbe, B. O. Bolaji, M. U. Olanipekun, and M. R. Adu, "Development of a solar photovoltaic power system to generate electricity for office appliances," *Engineering Journal*, vol. 17, no. 1, pp. 29–39, Jan. 2013.

[19] L. K. Biswas, M. H. Rahman, and S. Haque, "A low cost characteristics analyzer of PV module," in *Proc. International Conf. on Developments in Renewable Energy Technology (ICDRET)*, Dhaka, Jan. 2012, pp. 1–5.

[20] L. Hassaine, A. Mraoui, and M. Khelif, "Low cost electronic load for out-door testing of photovoltaic panels," *International Renewable Energy Congress (IREC)*, Hammamet, Mar. 2014, pp. 1–6.

[21] Avant! Coporation, "Using diodes" in *Star-Hspice Manual*, , release 1998.2, Jul. 1998, ch. 13.